Modelling and performance of conformal automotive antennas

L. Low, R. Langley and J.C. Batchelor

Modelling and performance of conformal automotive antennas

L. Low, R. Langley and J.C. Batchelor

Abstract:

The modelling of an automotive antenna printed on a glass window is described. Simulations are compared with measurements to verify the model at 100 MHz. Simulations include the entire external car body generated from mechanical CAD data and transformed into an appropriate electromagnetic model. The feed position, element design and antenna orientation for optimum gain are investigated. Surface current distributions over the vehicle are illustrated for different antenna positions. Simulated and measured radiation patterns are acceptable for prototype antenna design.

1.0 Introduction:

Advanced electromagnetic simulation tools and modern computers have opened up areas where analysis and modelling were beyond most expectations only 10 years ago. One such area is the design and simulation of hidden antennas on automobiles where the complexity and size of the vehicle even at relatively low frequencies present a very demanding electromagnetic analysis problem. Owing to the high costs involved in developing and measuring antenna performance on a vehicle, it is highly desirable to be able to rely on simulation tools. There are many locations in which low frequency antennas can be placed on an automobile but in most cases the glass window areas are used. Several studies have reported modelling studies for this type of antenna [1–7] using methods ranging from geometric optics to the method of moments and time-domain techniques. Many of these studies used simplified body shapes lacking design detail and omitted the glass substrates supporting the antennas. In higher specification automobiles, an antenna diversity system is often used with either two or four hidden antennas [8], as printing the antennas on glass inevitably reduces their individual performance when compared with a roof mount monopole. However, to keep costs down, a single hidden antenna is deployed on many lower range cars. The performance of a single active antenna can be improved by employing switched parasitic antennas whose load phasing can be varied [9]. An alternative diversity antenna was reported in [10] where a planar printed antenna was placed under a plastic panel in the roof of a vehicle. Other studies have focused on higher-frequency antenna performance on vehicles [11–14] where modelling the complete automobile becomes a formidable problem.

This paper describes the performance and simulation of a side window glass-based antenna for operation across the FM frequency band from 88 to 108 MHz. This type of antenna is commonly employed on 4 _ 4 sports utility vehicles and estate cars. The antenna geometry is simple and the antenna is often part of a diversity system with other antennas on the opposing quarter window and the rear window. The glass windows are included in the model as they affect the impedance match and antenna resonant frequency, and cause signal scattering. The antenna is fed using an unscreened flying lead from a matched amplifier as it is customary in automotive systems. This introduces some uncertainty into impedance measurements and the modelling of the port due to the variable routing of the wire during assembly. For this reason, the agreement between simulation and measurement of the impedance of vehicle antennas tends to be poor as noted in several papers [3, 6, 10]. The car used in this work was a Volvo V70 estate car (see Fig. 1), where the rear quarter window and antenna are clearly seen. The A, B, C and D pillars on the body are labelled.

This paper examines the geometry of the antenna and compares simulation results with measurements. The importance of the feed location and antenna orientation are analysed with respect to the overall antenna radiation performance and polarisation properties. The model of the body shell used in the simulations was derived from CAD data and refined into a suitable detailed electromagnetic model as shown in Fig.1. The model was composed of the external panels with internal components such as inner door skins, steering mechanism and internal furnishings omitted to keep the simulation problem as simple as possible. CST Microwave studio was used as the simulation software, which is based on the finite integration timedomain method. The direct importation of CATIA model data for the car components into Microwave Studio has proven to be problematic. Detail in the CATIA model data of a complete vehicle without engine parts supplied by the manufacturer estimated at 4–5 GB. When the major metallic parts are selected, this reduces to 400–500 MB and is still far in excess of requirements for electromagnetic modelling even with some simplification. The numerous surfaces must be meshed into a coherent electromagnetic model that can be handled by the simulator. These factors require that the car geometry must be simplified to a greater or lesser degree. Simplification can be attained by reducing the number of faces either by altering the geometry using the original CAD software that was used to create the geometry or an alternative CAE package such as CADFix or FEMAP. The data file for the whole car model was reduced from around 500 to 40 MB to produce a detailed electromagnetic structure which is far more manageable (see Fig. 2). The car was measured on the outdoor vehicle test range at Harada Industries Research Centre in the UK. This is a far field measurement range of 75 m long. The car is rotated on a metal turntable of 6 m in diameter. The transmitter source log periodic antenna is located at a height of 3 m on a mast and can be switched between horizontal and vertical polarisation.

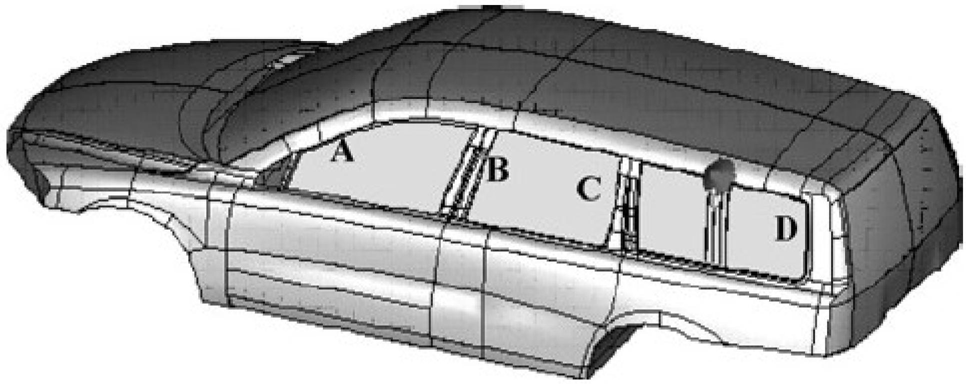

Fig. 1 *Car with the side quarter window antenna*
A, B, C, D pillars are labelled

2 Antenna geometry

Fig. 3 shows the geometry of the antenna and its dimensions in the window aperture. The antenna has four elements and is fed from the top using an unscreened flying lead from a matched amplifier. The antenna was printed using highly conducting ink of 1.5-mm width and was modelled as wires with perfect conductivity. Wires were used instead of fine slanted striplines in CST Microwave Studio as they are not prone to critical cell expansion; where a critical cell is when it is completely filled with a perfect conductor. The glass was 3-mm thick with a relative ε_r of 6.75 and loss tangent of 0.02. The antenna was printed on the inside face of the glass. The input impedance study here concentrates on the simulated antenna performance. Measurements of the resonant frequency were within 5% of the simulations and show the same bandwidth broadening as the number of elements was increased.

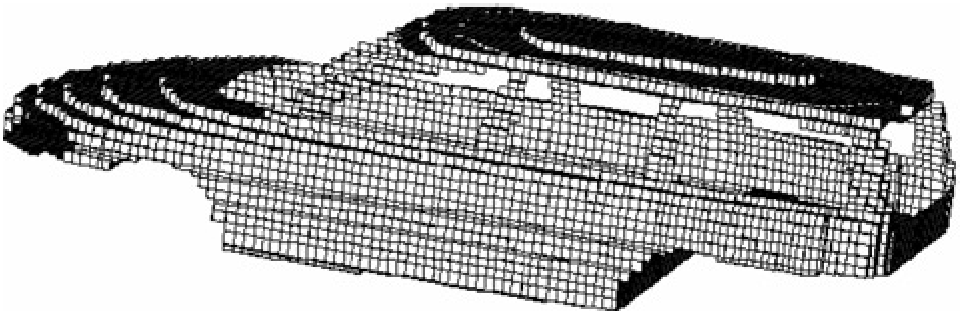

Fig. 2 *Vehicle grid model derived from CAD data*

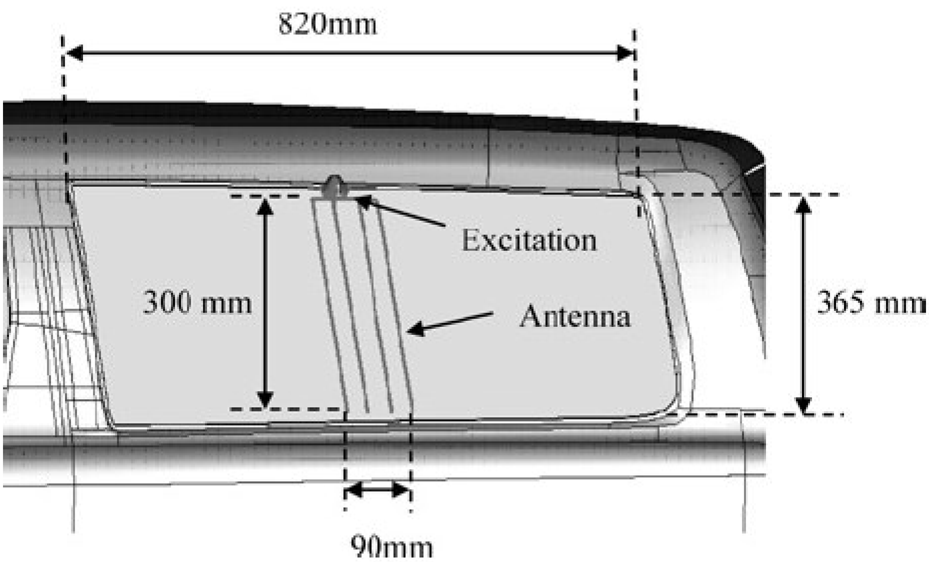

Fig. 3 *Geometry of the rear quarter side window antenna fed from top*

It is interesting to note that the size of the window aperture is in the region of a quarter wavelength and that the lengths of the vertical elements are very much shorter than the required quarter-wave monopole antennas in the FM band. The quarter wave antenna length should be about 530 mm for the upper frequency band at 108 MHz. However, the vertical elements of the antenna as shown in Fig. 3 are

316-mm long, too short to be resonant in the FM band and there is substantial and complex coupling between the antenna element and the vehicle window aperture which will be discussed later. It is desirable for the FM antenna to occupy the least area possible so that other communication antennas such as TV, keyless entry and digital audio band antenna can be mounted on the same glass area. The antenna in Fig. 3 has four linked monopole elements and the investigation started by examining the monopole antenna and changing the number of elements from 1 to 4. Fig. 4 shows the simulated return loss for the antenna with one, two, three and four elements forming the monopole. It is seen that the bandwidth for a single-element monopole was narrow and the resonance was higher than the top end of the FM band at 115 MHz. As the number of elements is increased, so the resonant frequency was reduced and the bandwidth increased. With four elements, the antenna has a good impedance bandwidth over the entire FM band (88–108 MHz), the return loss was 28 dB or better which is good for a glass-based FM broadcast reception system. There are two strong resonances at both ends of the FM band, that is, from Fig. 4 at 86 and 105 MHz, that combine to provide a broad impedance bandwidth. The return loss is sensitive to the spacing between the roof of the vehicle and the horizontal element of the antenna. In this case, the distance from the top of the roof to the horizontal element of the antenna was 30 mm. Reducing the number of elements simply reduces the bandwidth but it would be possible to use three elements if necessary.

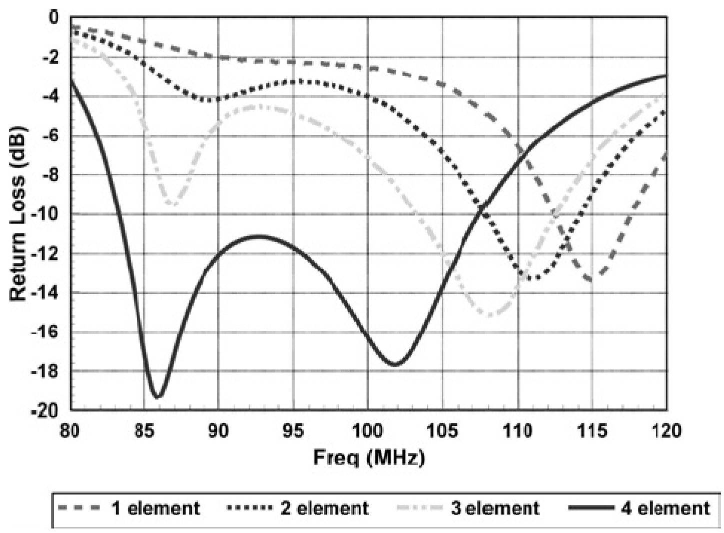

Fig. 4 *Simulated return loss of the antenna system with variable number of slanted vertical strips*

3 Radiation patterns

The azimuth radiation patterns of the four-element configured quarter window antenna have been computed and measured. In general, a vehicle will receive signals from some distance, and the azimuth plane gives a good indication of received power performance at the car antenna. The gains of the side window antennas have been compared with a reference monopole antenna mounted at the centre of the roof [10]. The measured gain for the reference monopole was 1.0 dBi vertical polarisation, 210.9 dBi horizontal polarisation, whereas the measured gain for the side window antenna was 23.9 and 28.2 dBi, respectively. The measured azimuth radiation patterns were taken over the entire FM band on the open site facility with low interfering signal levels from surrounding FM broadcast transmitters. As an example, the measured and simulated vertical and horizontal radiation pattern plots taken at 100 and 107 MHz are compared in Fig. 5. The radiation patterns for 88 MHz are discussed in a later section. Fig. 5 shows typical plots and demonstrates the ability of the model to predict the radiation performance. The absolute power levels between the measured and computed radiation patterns are arbitrary and the following comparisons are made on the basis of shape rather than power level.

For the case of 100 MHz, the general omni-directional shape of the vertical polarisation pattern in Fig. 5a is better predicted than the more complex horizontal pattern in Fig. 5b, in particular, the nulls towards the rear of the car. Similar comments can be made for the patterns at 107 MHz. There was more radiation towards the rear of the car for vertical polarisation (Fig. 5c) at this frequency than at 100 MHz, whereas the prediction of the nulls in the horizontal patterns in Fig. 5d was good at some angles and not others. In general, it can be extremely difficult to predict accurately the position of the nulls. Nulls are caused by cancellation of two near-identical signal components, and very small changes can cause large changes in the behaviour of the nulls. The impact of all the internal furnishings on the radiation patterns is being determined in a follow on study but early indications show that the seats are particularly important within the car body cavity and affect the radiation pattern nulls. Although the agreement between the measured data and the predicted radiation patterns is not perfect, it is sufficiently accurate for initial design purposes. Nulls are also predicted in the correct positions in many cases.

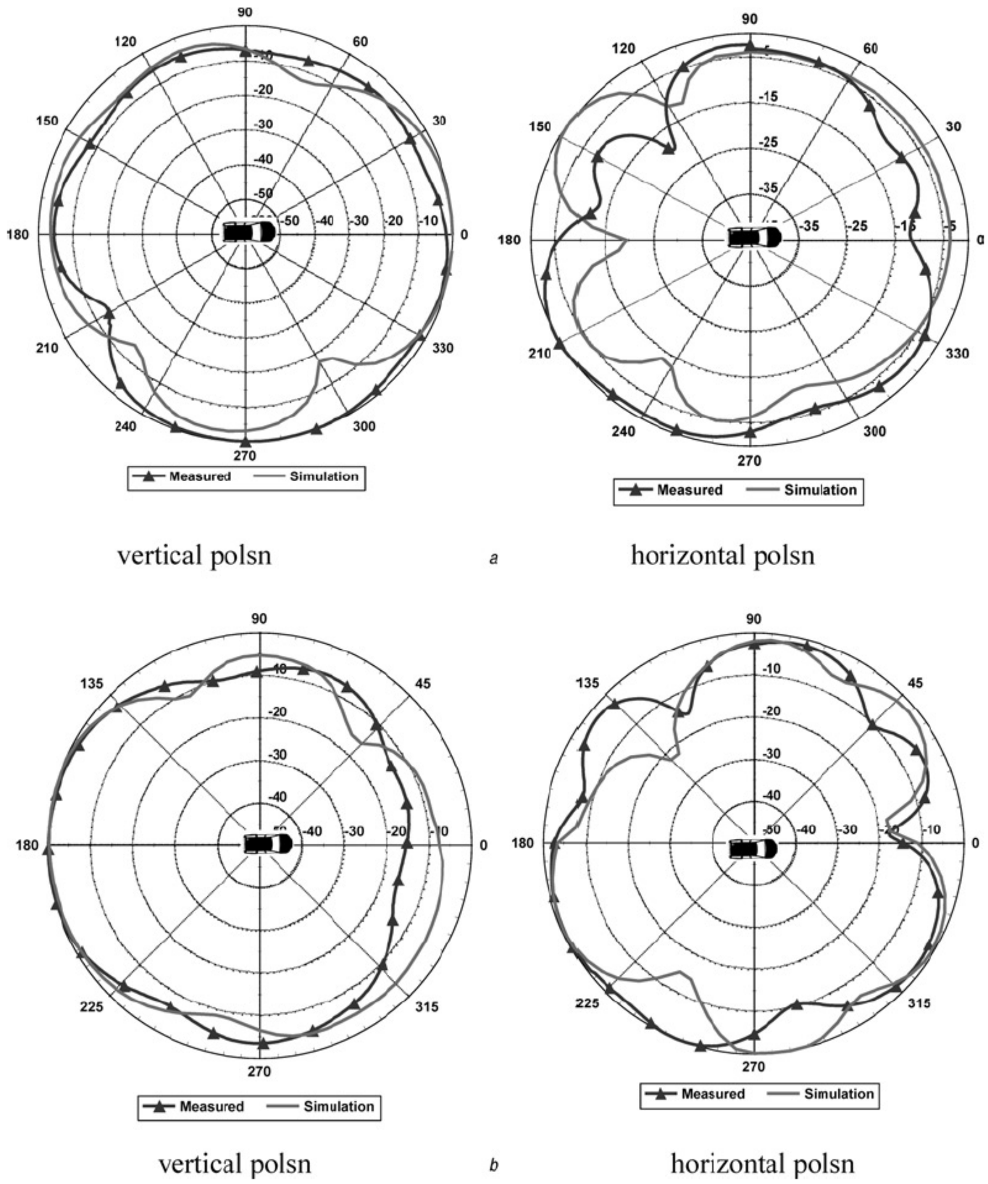

Fig. 5 *Simulated and measured radiation patterns for the window antenna*
a At 100 MHz
b At 107 MHz
■ Measured
— Simulated

4 Polarisation performance

It is desirable for vehicular FM broadcast reception antennas to receive in both polarisations for a number of reasons. For example, vertical polarisation is predominantly broadcast in the UK, whereas in the rest of continental Europe horizontal polarisation is widely used. In the USA, either slant 458 linear or circular polarisation is used. In addition, the configuration is useful for the reception of broadcast signals when the polarisation of the transmitted signal is changed due to multipath and ground reflections. For a mast antenna and for antennas in large apertures, it is often possible to slant the antenna from a vertical position to improve the horizontal polarisation performance at the expense of the vertical so that the received power levels are within about 7 dB. However, this may not always be achievable when the antenna is placed in a confined space as in the case of the quarter window antenna where changing the slant angle of the antenna has no significant effect on the respective polarisation gains because of the fact that it is exciting an aperture and body currents on the car rather than the antenna element. In the case of the side window antenna, the difference in the measured power levels between the vertical and horizontal polarisation varied across the frequency band from 28 to 213 dB.

5 Effect of varying antenna feed position

There are many possible locations where the antenna can be fed on the quarter window. The feed point may be specified by the manufacturer due to the proximity of airbags and actuators, other electronics and so on. However, as the antenna performance is critical in a confined space we have examined the performance of the antenna as the feed point was varied. Using numerical simulation, this section investigates how the feed position of the antenna can affect the power received by the antenna. The same basic antenna structure was used for the various feed locations but the lengths and slant of the elements were modified for optimal impedance match at each feed location. Fig. 6 shows the various feed locations on the quarter window that were used, and the actual feed position was chosen to give a reasonable impedance match. In addition, an 80-cm long monopole antenna positioned on the car roof at its centre was simulated as a reference antenna for comparison. The results presented are derived from the simulated radiation patterns at a frequency of 90 MHz which is representative of the overall performance of the antennas. An error bar graph format is employed to show the average radiated power from the antenna, together with the minimum and maximum radiated levels. The average maximum and minimum power levels for vertical and horizontal polarisation for the various feed positions are plotted in Fig. 7. Readings were taken over 360° in the azimuth plane, and the power levels are normalised to the maximum value of a vertically polarised component of the whip monopole antenna placed at the centre of the roof.

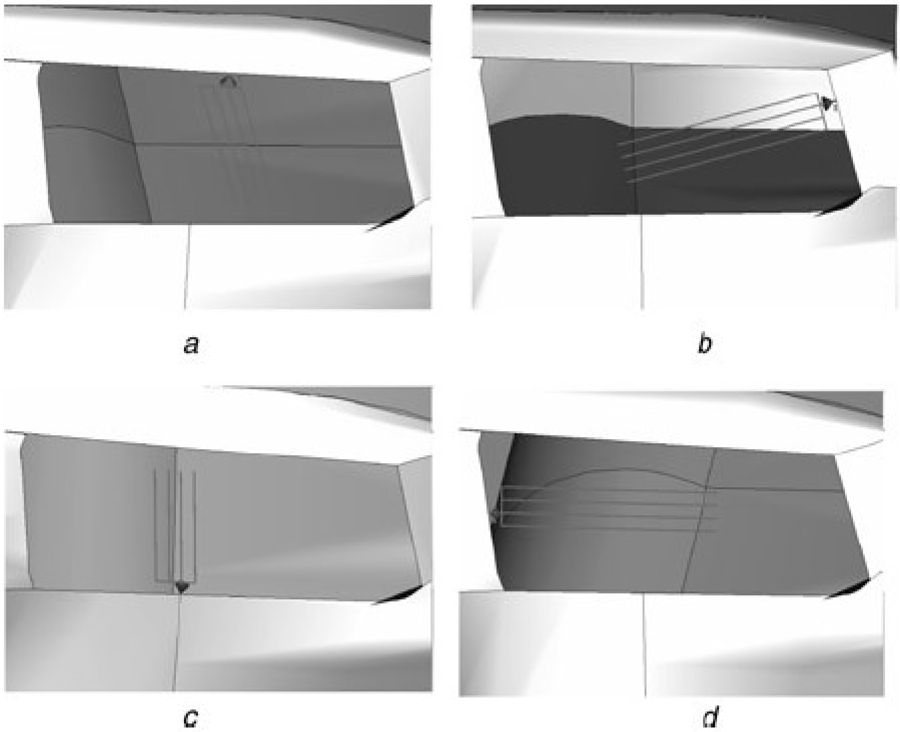

Fig. 6 *Experimental setup for various feed point locations*
a Top
b D pillar
c Bottom
d C pillar

This gives a reference to the performance of the antenna compared with a roof antenna. The difference between the maximum and minimum values gives an approximated indication of the omnidirectional properties of the patterns. A small difference between the values represents a pattern that is relatively omni-directional and a large difference (.10 dB) indicates that a strong null is present in the radiation plot. Nulls are important for diversity systems but are a problem if a single antenna receiving system is used. Fig. 7 shows that the minimum difference in nulls in both polarisations is more than 10 dB and is particularly variant for horizontal polarisation. Hence, all feed locations are suitable for implementation in a diversity system where patterns' nulls are important. Comparing the vertical polarisation component of the antenna at feed position 1 (top fed) of the quarter window to the reference whip monopole antenna, Fig. 7a shows that there is a difference in max radiated power level of less than 1 dB and on average it was just 5 dB lower, a strong performance for a hidden antenna. For feed positions 2 and 3, a difference in average power level of 8–9 dB below the roof monopole was recorded, whereas at feed position 4 the average level was 22 dB down, much of the power being radiated into other planes. It is typical for a vertical polarised component of a whip monopole antenna to be 7–10 dB stronger than the horizontally polarised component. From Fig. 7b, it can be seen that the horizontal polarisation performance of the antenna at feed position 2 was strongest, closely followed by position 1 with feed positions 3 and 4 having low average power levels although very high variations between maximum and minimum power levels. Overall, it might be concluded that the original feed position 1 or position 2 has optimum performance for non-diversity operation. The radiation patterns of the antenna when fed in the different locations are shown in Fig. 8. The patterns are normalised to 0 dB. The patterns show that the feed position significantly affects the shape of the radiation pattern and the positions of nulls generated especially so for horizontal polarisation. The results for feed position 1 have the best overall symmetry for reception but perhaps position 4 provides most diversity reception possibilities when combined with other antennas as it shows both diversity in the position of the nulls and significant power level changes (.15 dB) in azimuth around the car.

6 Surface current analysis Fig. 9 shows the current induced in the vehicle body at 90 MHz by the quarter window antenna when it was fed in various positions around the quarter window. When the antenna was fed on the top of the quarter window, there are strong currents around the C and D pillars (see Fig. 1) surrounding the glass. The currents extend from the C pillar towards the rear wheel arch and are uniform on the top rim of the window. Currents are also induced on the A and B pillars with a weak standing-wave-type current pattern on the bonnet. Comparing the radiation plots with the currents, it is interesting to note that these strong currents add constructively at 90 MHz to form an almost omnidirectional pattern in the vertical polarisation and has created nulls at 90° and 180° in the horizontal polarisation. When the antenna feed position is changed from the top feed to the bottom feed, Fig. 9c shows that the currents on the roof area above the window

were no longer uniform and that the surface currents do not extend to the wheel arch.

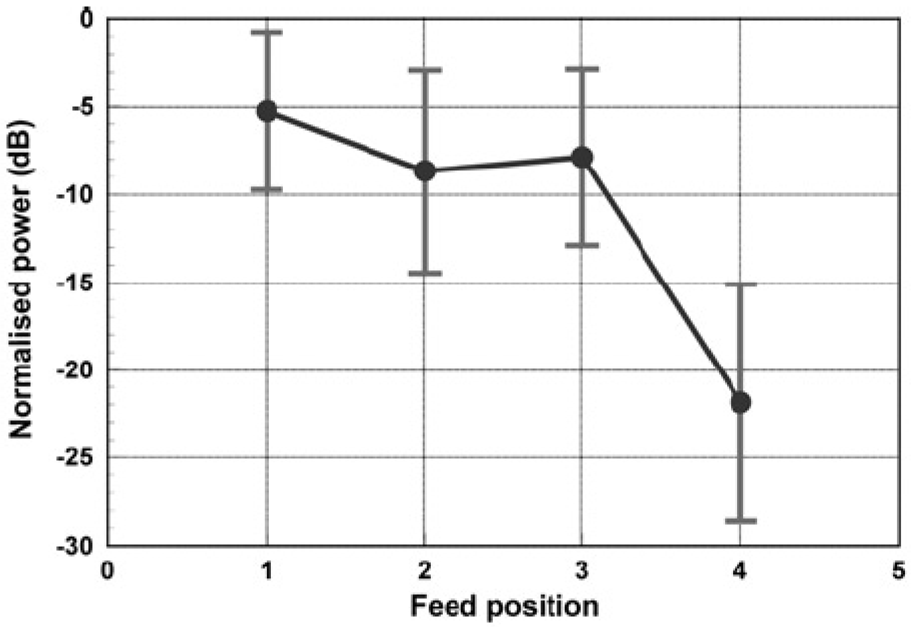

a

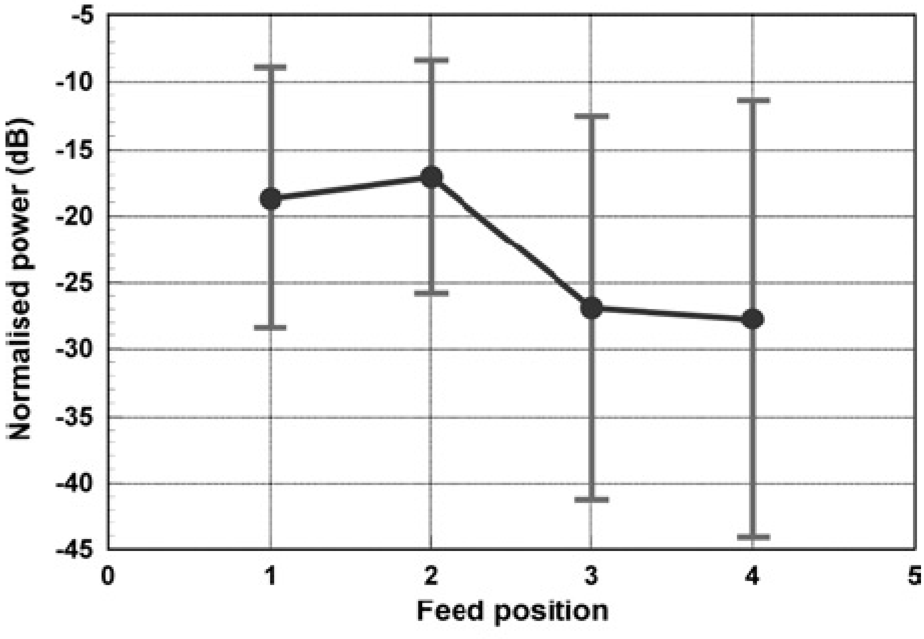

b

Fig. 7 *Normalised power for various feed positions at 98 MHz*
a Vertical polarisation
b Horizontal polarisation

Instead, there is a uniform current being induced at the bottom rim of the quarter window. This is expected as there should be high current flow around the region of the feed. The vertical radiation pattern remains somewhat omni-directional but the pattern in the horizontal polarisation has an additional null at 120° and the nulls at 90° and 180° are shifted by about 20° anti-clockwise. This change in current distribution around the aperture has resulted in a change in radiation pattern as expected. The current distribution when the antenna was fed on the C and D pillars are very different from that of the top and bottom fed positions. High current densities are not found on the A and B pillars, and the standing wave on the bonnet is not present (see Figs. 9b and d). This has created a different radiation plot from the case of the top and bottom feed configurations. This observation shows that currents on the pillars contribute to radiation in both horizontal and vertical polarisations.

7 Conclusion

The performance of a quarter-window-based hidden automotive antenna operating near 100 MHz has been analysed both for diversity operation and when used as a single antenna. The simulated radiation patterns were in reasonable agreement with those measured, although some nulls were not predicted and there were significant discrepancies in pattern levels of more than 10 dB at some angles.
Nevertheless, the simulations were certainly sufficiently accurate for initial antenna design and placement. It is extremely difficult to quantify the improvements made in predicting the radiation performance of the car antennas when a detailed body shell model is used as opposed to a simple planar panel model as the internal details also affect the simulations. A more advanced study yet to be completed shows that including the body detail provides a much closer agreement with measurements particularly in the prediction of nulls where the simplest model often fails to predict the majority of them. The antenna impedance is not significantly affected by the internal or external detail but depends heavily on the ability to model the environs of the feed including the simple non-RF connectors used between the amplifier and the glass. This issue remains to be addressed. In this case study, the matching and bandwidth of the antenna depend on the number of elements, with four elements giving acceptable performance with a return loss of better than 8 dB over the FM band. The position of the feed point and antenna orientation also affected the matching and bandwidth.

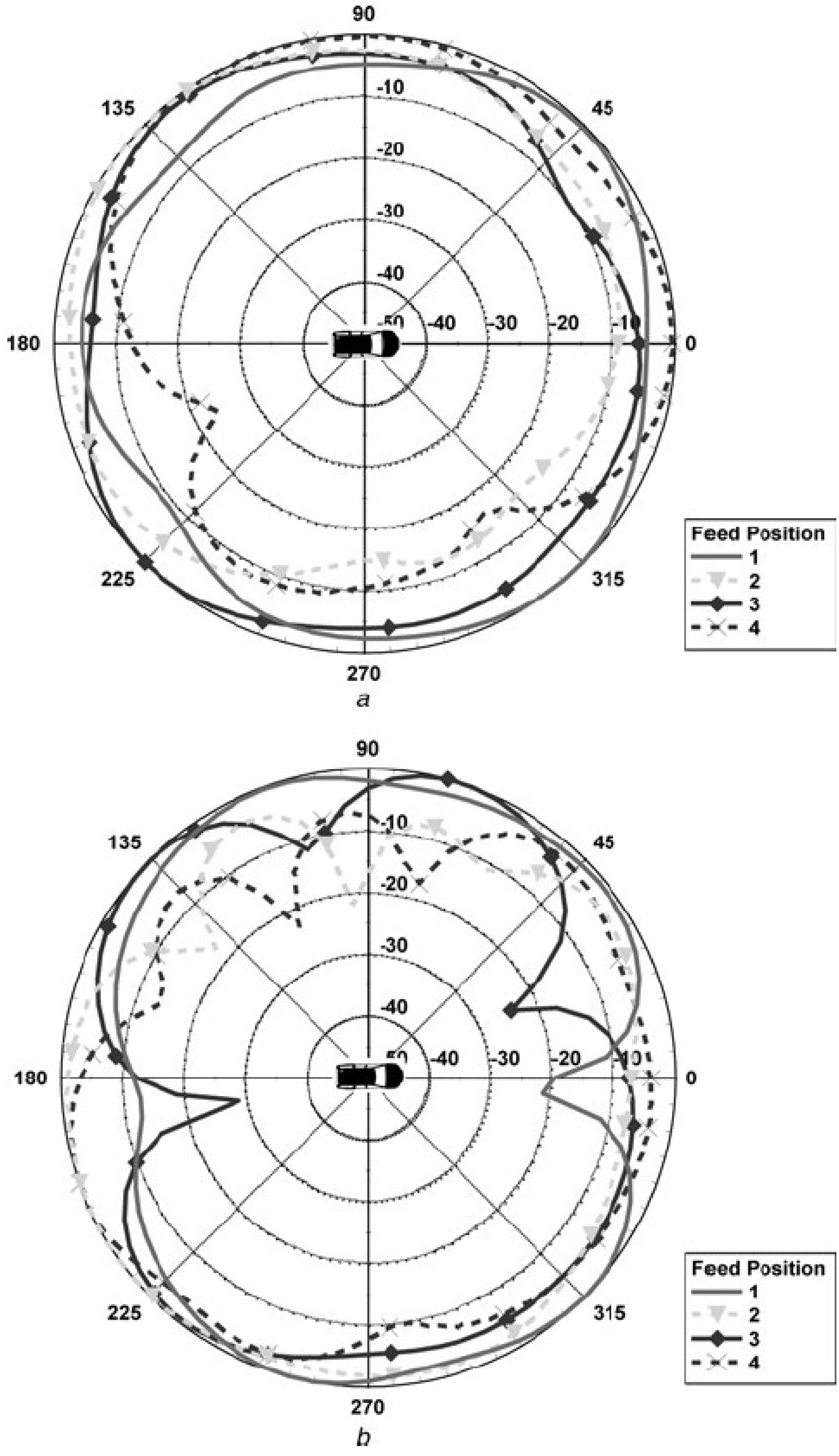

Fig. 8 *Radiation pattern for various feed positions at 90 MHz*

a Vertical polarisation
b Horizontal polarisation

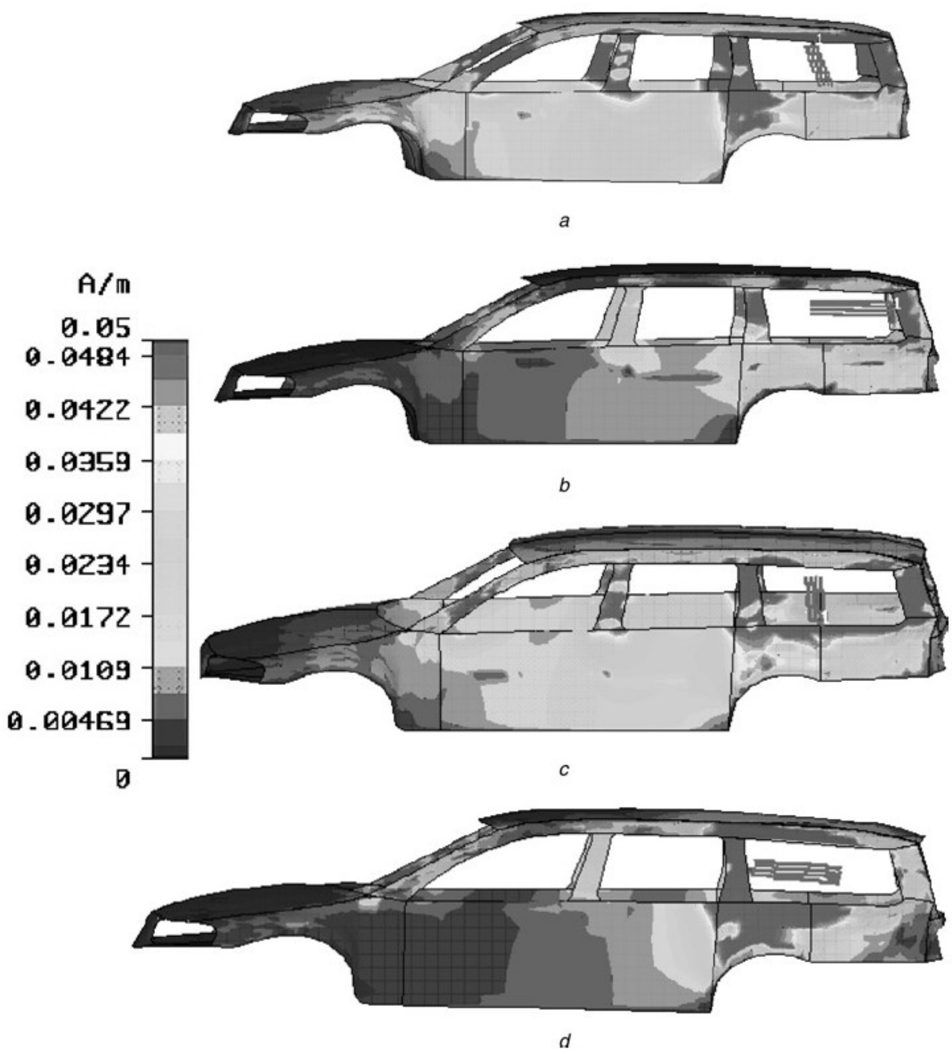

Fig. 9 *Surface currents induced on a car body by the quarter window antenna fed in various positions*
a Top
b D pillar
c Bottom
d C pillar

Measurements and simulations in the azimuth plane showed that feeding the antenna from the top of the car (roof) produced good overall performance as did feeding it from the D pillar at the rear of the car. The single antenna had an average gain just 5 dB lower than a roof-mounted quarter wave mast antenna, good for a hidden antenna. Turning the antenna over and feeding it from below resulted in much reduced sensitivity of about 10 dB, whereas feeding from the C pillar again resulted in lower gain but pattern diversity was enhanced, showing that diverse radiation patterns could be produced by changing the feed position. Overall simulations proved a valuable tool in antenna design and evaluation on the vehicle.

8 Acknowledgments

The authors thank Volvo Cars, Sweden, and Harada Industries Ltd. for supplying CAD data and antenna measurements for this study.

9 References

1 Austin, B.A., and Najm, R.K.: 'Conformal on-glass vehicle antennas at VHF'. IEE Int. Conf. Antenna and Propag. (ICAP), 1993, vol. 2, pp. 900–903

2 Ehmann, R., Wagner, B., and Weiland, T.: 'Farfield calculations for car antennas at different locations', IEEE Trans. Magn., 1997, 33, (2), pp. 1508–1511

3 Abou-Jaoude, R., and Walton, E.K.: 'Numerical modelling of on-glass conformal automobile antennas', IEEE Trans. Antennas Propag., 1998, 46, (6), pp. 845–852

4 Walton, E.K., and Abou-Jaoude, R.: 'Annular slot windshield antenna', IEEE Trans. Veh. Technol., 1998, 47, (3), pp. 766–773

5 Jakobus, U.: 'Efficient techniques for modelling integrated windscreen antennas within the method of moments'. Millennium Conf. Antennas and Propag., Davos, Switzerland, April 2000, pp. 102–105

6 Batchelor, J.C., Langley, R.J., and Endo, H.: 'On-glass mobile antenna performance modelling', IEE Proc., Microw. Antennas Propag., 2001, 184, (4), pp. 233–238

7 Low, L., and Langley, R.J.: 'Modelling automotive antennas'. IEEE Antenna Propag. Int. Symp. 2004, vol. 3, pp. 3171–3174

8 Fujimoto, K., and James, J.R.: 'Mobile antenna system handbook' (Artech House, Norwood, MA, 1994)

9 Low, L., and Langley, R.J.: 'Single feed antenna with radiation pattern diversity', Electron. Lett., 2004, 40, (16), pp. 975–976

10 Low, L., and Langley, R.J.: 'Hidden automotive antenna performance and simulation', IEEE Trans. Antennas Propag., 2006, 54, (12), pp. 3707–3712

11 Ali, M., Yang, G., and Hwang, H.S.: 'Design and analysis of an R-shaped dual-band planar inverted-F antenna for vehicular applications', IEEE Trans. Veh. Technol., 2004, 53, pp. 29–37

12 Clasen, G., and Langley, R.J.: 'Meshed patch antennas', IEEE Trans. Antennas Propag., 2004, 52, pp. 1412–1416

13 Song, H.J., Hsu, H.P., Wiese, R., and Talty, T.: ‘Modelling signal strength range of tyre pressure monitoring systems in automobiles’. IEEE Antenna Propag. Int. Symp. 2004, vol. 3, pp. 3167–3170
14 Leelaratne, R., and Langley, R.: ‘Multiband PIFA vehicle telematics antennas’, IEEE Trans. Veh. Technol., 2005, 54, (2), pp. 477–485